

Distribution of Hydrophobic Probe Molecules in Lipid Bilayers. 2. Time-Resolved Fluorescence Anisotropy Study of Perylene in Vesicles

M. A. M. J. van Zandvoort,^{*,†,‡} H. C. Gerritsen,[‡] G. van Ginkel,[‡] Y. K. Levine,[‡] R. Tarroni,[§] and C. Zannoni[§]

Department of Molecular Biophysics, Debye Institute, Buys Ballot Laboratory, Utrecht University, P.O. Box 80000, 3508 TA Utrecht, The Netherlands, and Dipartimento di Chimica Fisica ed Inorganica, Università degli studi di Bologna, Viale Risorgimento 4, 40136 Bologna, Italy

Received: October 31, 1996; In Final Form: February 19, 1997[⊗]

The orientational distribution and rotational dynamics of planar perylene molecules incorporated into spherical vesicles of palmitoyl- δ -9-oleoyl(16:0,18:1)phosphatidylcholine (POPC) was studied using time-resolved fluorescence anisotropy. The experimental anisotropy decay curves were analyzed using a global target approach. Here, anisotropy curves obtained at six temperatures above the gel–lamellar phase transition of the vesicles as well as the two combinations of excitation and emission wavelengths, (256, 470 nm) and (410, 470 nm), were fitted simultaneously. We have utilized two sets of orientational distributions of perylene in the bilayer. One set contains various one-population orientational distributions, while the other consists of models in which the probes are distributed over two distinct orientational populations. We find that in general the models yield statistically equivalent solutions, though the two-population models need a substantially smaller number of fit parameters. The existence of two distinct orientational populations of perylene in the lipid vesicle bilayer is in agreement with the results of Monte Carlo dynamics simulations in the preceding paper, but we argue that additional independent information is needed in order to remove the remaining ambiguities. We conclude that time-resolved anisotropy experiments on macroscopically unoriented samples do not provide sufficient information in order to fully characterize the orientational distribution of probe molecules in the bilayers.

Introduction

The physical properties of artificial, pure lipid structures provide many needed insights into the functioning of membrane systems in living organisms. The orientational and dynamic behavior of lipid structures such as monolayers, bilayers, and vesicles is a key aspect in building up the picture. This behavior is frequently monitored with fluorescent probes incorporated in the lipid structures at low concentrations. Commonly, probes such as 1,6-diphenyl-1,3,5-hexatriene (DPH), its polar analogue 1-(4-trimethylammonio)-DPH (TMA-DPH), and perylene^{1–27} are used. The information about the static (structural micro-heterogeneity, polarity, orientation) and the dynamic (especially nanosecond reorientations) properties of the surrounding lipids can be obtained from observables such as the fluorescence lifetime and fluorescence anisotropy.²⁸

The extraction of information about order and dynamics in spherical vesicles from fluorescence anisotropy decays is hampered by the intrinsic ambiguity of the analysis.^{29,30} This stems from the fact that the experimental anisotropy signal is a sum of three independent second-rank orientational correlation functions and cannot be resolved unequivocally into its individual contributions. It has been amply demonstrated that although many physically distinct models for the orientational order and dynamics provide excellent fits to the anisotropy decay,^{31–37} only few describe correctly the separate correlation functions.^{35,38–40} The analysis of the anisotropy decay curves thus can only be carried out if additional independent information is available.

Recently, this has been addressed in a study on the distribution of DPH in vesicles of various unsaturated lipids.⁴¹ The time-resolved polarized fluorescence experiments were linked to the dependence of the lifetime of DPH on the polarity of the surrounding medium and thus on its position of the probe in the bilayer. The analysis revealed that at least two populations of DPH molecules are present in the bilayer, each possessing a characteristic orientational and dynamical behavior. This is not the result of the coexistence of gel and bilayer phases but rather of a competition between the interactions between the DPH molecules and the lipid chains on one hand and their tendency to partition into the center of the bilayer on the other. It is important to realize that the center of the bilayer is a region with considerable free volume as the result of the imperfect packing of the lipid chains belonging to the two opposing monolayers.⁴¹ Similarly, a two-population model was invoked in order to account for the fluorescence depolarization of DPH in columnar liquid crystals, where it is found to partition between the core and chain regions.⁴²

In the preceding paper Monte Carlo dynamics (MCD) simulations are used to demonstrate how two populations of nonanchored probe molecules such as DPH and perylene can arise within a lipid bilayer. It is shown that the tendency of these molecules to access the regions of free volume at the center of the bilayer can be counteracted by invoking a repulsive potential, the so-called burial potential. This potential results in a distribution of the centers of mass of the probes over the thickness of the bilayer. The distribution may be described as a dynamic equilibrium between two population sites, each possessing distinct orientational and dynamical behavior.

The simulations also show that the analysis of anisotropy decays from such a heterogeneous system is inherently ambiguous. The anisotropy decays can be fitted satisfactorily using

* Corresponding author.

[†] Utrecht University and Università degli studi di Bologna.

[‡] Utrecht University.

[§] Università degli studi di Bologna.

[⊗] Abstract published in *Advance ACS Abstracts*, April 1, 1997.

many different single-population models, as well as two-population ones. We have argued that in the case of DPH, the ambiguity can be removed by exploiting the dependence of the fluorescence lifetime on polarity and thus the location of the probes in the bilayer structure, in agreement with the findings in ref 41. In marked contrast, the fluorescence intensity decay of perylene is almost insensitive to polarity,^{43–47} so the ambiguity in the analysis remains.

Here, we shall address the question as to whether the ambiguity in the analysis of the anisotropy decay of perylene can be circumvented by the use of global target analysis (GTA) techniques.⁴⁸ To this end we have carried out an experimental study of the time-resolved anisotropy of perylene in palmitoyl- δ -9-oleoyl(16:0,18:1)phosphatidylcholine (POPC) vesicles at different temperatures by exciting at both absorption bands. The experimental data were analyzed with two different sets of models. One set contains various one-population orientational distributions of the perylene molecules in the vesicle membrane, while the second set consists of models in which the probes are distributed over two distinct orientational populations. In both sets the Brownian rotational diffusion (BRD) model was used to describe the reorientational dynamics of the probes.

We find that that both sets of models yield statistically equivalent fits. However, the two-population models require a significantly smaller number of fit parameters than the single-population ones. The two-population models indicate that the majority of perylene molecules ($\sim 90\%$) are intercalated between the lipid tails, while the remaining 10% are unoriented and located in the middle of the layer. Nevertheless, the simulations presented in the preceding paper show that this division into an oriented and an unoriented population may well be an artifact of the analysis.

We conclude that it is indeed highly likely that perylene molecules are present as two populations in the bilayer. These populations have different orientational and reorientational properties. Since, however, no independent information about the exact distribution of the molecules over the bilayer is available, the results of the global target analysis remain ambiguous.

Experimental Section

Sample Preparation. Perylene was obtained from Fluka AG and used without further purification. POPC (palmitoyl- δ -9-oleoyl(16:0,18:1)phosphatidylcholine) was purchased from Sigma Chemical Company (St. Louis, MO). The perylene-POPC vesicles (1:500) were prepared as described previously.⁴ All samples exhibited the typical monomeric perylene absorption and fluorescence spectra.^{49–52}

Experiments. The time-resolved anisotropy decay measurements were carried out using the synchrotron radiation source (SRS) in Daresbury, U.K. operating in the single bunch mode as a tunable light source with high repetition frequency (3 MHz). The excitation wavelength (either 256 or 410 nm) was selected with a monochromator (bandwidth of 0.1–1 nm). The macroscopically isotropic vesicle suspension in a quartz cuvette (path length of 1 cm, absorbance below 0.1) was then excited with a short (fwhm = 200 ps) pulse of vertically (V) polarized light using a Glan-Taylor prism as the polarizer. The complete setup is described elsewhere.⁵³ The fluorescence emission was detected with a 90° scattering geometry using a standard single-photon counting system with vertical (V) and horizontal (H) polarization directions. The anisotropy $r(t)$ is now defined as

$$r(t) = \frac{I_{VV}(t) - I_{VH}(t)}{F(t)} \quad (1)$$

where $F(t) = I_{VV}(t) + 2I_{VH}(t)$ is the fluorescence intensity decay.

The emission wavelength (470 nm) was selected and scattering by the emitted light was avoided by passing the light through a narrow band interference filter in combination with a cutoff filter. The absence of stray light was checked prior to any measurement, and a pulse profile was obtained from scattering by Ludox. The correction factor $G(=I_{HH}/I_{HV})$ accounting for the differential in response to the photomultiplier tube (Philips XP2020Q) to horizontally and vertically polarized light was determined using a dilute perylene/ethanol solution and found to be 1.00 ± 0.01 .

The time-dependent intensities $I_{VV}(t)$ and $I_{VH}(t)$ were measured at six temperatures (10, 15, 20, 25, 30, and 35 °C) above the gel-lamellar phase transition of the POPC vesicles. At each temperature the intensities were measured using two combinations of excitation and emission wavelengths: (256, 470 nm) and (410, 470 nm). This resulted in a total of 24 intensity decay curves with a common emission polarization direction.

Fit Procedures. The intrinsic ambiguity in the analysis of the anisotropy decay can be significantly reduced by fitting simultaneously the intensity decays at all six temperatures using the GTA approach.⁴⁸ This involves the calculation of $r(t)$ and $F(t)$ using a given set of adjustable model parameters followed by the evaluation of $I_{VV}(t)$ and $I_{VH}(t)$. The model parameters are then optimized to obtain the best agreement between the calculated and experimental intensities. This involves an intermediate step of convoluting the calculated intensity decays with the measured instrumental response function. Furthermore, a time shift is introduced as a fit parameter in order to compensate for the differences in photomultiplier transit times for electrons emitted at the cathode by light with different wavelength and polarization.

The quality of the measurements and the lowest χ^2 possible were judged by a model-free analysis in which $r(t)$ and $F(t)$ at each temperature and combination of excitation and emission wavelengths were fitted separately to a multiexponential decay function. It turned out that the total intensity decay could be excellently described by a single exponential at all temperatures:

$$F(t) = e^{-t/\tau(T)} \quad (2)$$

with τ depending on temperature T .

The deconvolution software package developed and described in ref 48, which implements a GTA with a modified Gauss-Newton-Marquardt nonlinear least-squares fitting, was used in the analysis. All calculations were run on an HP735 workstation.

Theory. The fluorescence anisotropy $r(t)$ reflects the orientational properties and the stochastic rotational dynamics of the perylene molecules in the lipid membrane. In spherical lipid vesicles it can be expressed as the sum of three correlation functions $G_k(t)$:⁴⁰

$$r(t) = 0.4[G_0(t) + 2G_1(t) + 2G_2(t)] \quad (3)$$

with

$$G_k(t) = \sum_{i,j,k=-2}^2 \langle D_{ki}^2(\Omega_{sm0}) D_{kj}^{2*}(\Omega_{smt}) \rangle D_{i0}^2(\Omega_{mu}) D_{j0}^{2*}(\Omega_{mv}) \quad (4)$$

Here, $D_{mn}^2(\Omega_{sm})$ are the Wigner rotation matrix elements of rank 2.⁵⁴ Ω_{sm0} and Ω_{smt} denote the three Euler angles characterizing the orientation of the molecule relative to the local bilayer normal at time $t = 0$ and t , respectively. Ω_{mu} and Ω_{mv} are the Euler angles of the absorption and emission dipole moment in the molecular frame, respectively. The brackets $\langle \dots \rangle$ denote an orientational average.

It can be readily shown⁴⁰ that $r(0)$, the limiting anisotropy at time $t = 0$, is determined by the angle δ between the excitation and emission transition dipole moments:

$$r(0) = 0.2(3 \cos^2 \delta - 1) \quad (5)$$

In spherical vesicle systems the anisotropy decays to a plateau at long times,¹ $t \rightarrow \infty$:

$$r(\infty) = \sum_{i,j=-2}^2 \langle D_{0i}^{2*}(\Omega_{sm}) \rangle \langle D_{0j}^2(\Omega_{sm}) \rangle D_{i0}^2(\Omega_{mv}) D_{j0}^{2*}(\Omega_{mv}) \quad (6)$$

where $\langle D_{0i}^2(\Omega_{sm}) \rangle$, the order parameters, are defined as averages over the Boltzmann distribution corresponding to the orienting potential $U(\Omega_{sm})$ experienced by the probe in the bilayer:

$$\langle D_{0i}^2(\Omega_{sm}) \rangle = \frac{\int d\Omega_{sm} D_{0i}^2(\Omega_{sm}) e^{-U(\Omega_{sm})/kT}}{\int d\Omega_{sm} e^{-U(\Omega_{sm})/kT}} \quad (7)$$

Knowledge of the order parameters can be used to reconstruct the orientational distribution function of the probes by using the maximum entropy approach.⁵⁶ However, it is important to note that not all order parameters can be accessed experimentally and that furthermore many are identically zero for reasons of symmetry.^{57,58}

The decay of the anisotropy due to reorientational dynamics of the probes in the vesicle bilayer can be described by the Brownian rotational diffusion model (BRD).^{33,35,59} In this model the molecules are assumed to undergo small-step stochastic rotational motions under the influence of the effective orienting potential $U(\Omega_{sm})$. The specific details of this model can be found elsewhere, while the effective potential $U(\Omega_{sm})$ employed will be discussed later on.

Consequently, the analysis of the fluorescence anisotropy decays yields information about the orientation of the transition dipole moments in the molecular frame and on the orientational and dynamical properties of the probes in the vesicle bilayer.

Basic Assumptions about Lipid Phase, Molecular Shape, BRD, and Potential. The perylene molecule (Figure 1) may be considered flat and to have a rectangular shape in both the excited and the ground state.⁶⁰ It is known that perylene has two separate excitation bands, one around 256 nm and one ranging from 390 to 440 nm. Steady-state anisotropy measurements indicate that the latter absorption band and the emission band are pure, while the 256 nm band may be taken to be pure to a good approximation.⁶⁰ The molecular z -axis is here chosen to be perpendicular to the molecular plane. Since the transition moments lie in the molecular plane, their orientations may be taken to be $\Omega_{mu} = \{\alpha_\mu, 90^\circ, 0^\circ\}$ and $\Omega_{mv} = \{\alpha_\nu, 90^\circ, 0^\circ\}$. We shall henceforth assume that this orientation is independent of temperature.

The rotational diffusion of the perylene molecule in the BRD model is described by two diffusional coefficients. The first (D_\perp) describes the reorientation of the molecular z -axis relative to the local bilayer normal, the so-called out-of-plane rotations. The second (D_\parallel) gives the in-plane rotations, the reorientation of the molecular plane around its molecular z -axis. Both D_\perp and D_\parallel will be taken to be dependent on temperature but independent of the excitation and emission wavelengths, since they are molecular shape properties.

The bilayer structure in a vesicle may be considered to be locally uniaxial and independent of the first Euler angle. We may thus set $\Omega_{sm} \equiv (\beta_{sm}, \gamma_{sm})$.^{40,57,58} We note that for the case

long symmetry axis

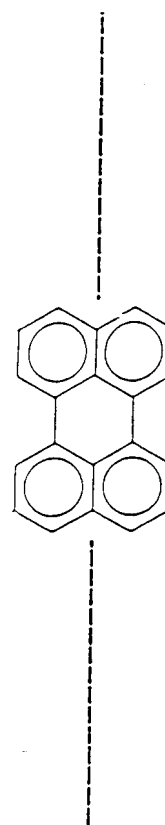


Figure 1. Molecular structure of perylene. The molecular z -axis is chosen perpendicular to the plane of the ring. The $S_0 \rightarrow S_1$ transition at 410 nm is generally believed to be located approximately along the long molecular axis, while the $S_0 \rightarrow S_4$ transition at 256 nm is oriented approximately along the short molecular axis.

of a cylindrically symmetric molecule Ω_{sm} becomes independent of the third Euler angle γ_{sm} .

The models for the rotational diffusion of the perylene molecules only differ in the form assumed for the orienting potential $U(\Omega_{sm})$. In general, the maximum entropy form of the potential will be taken to be

$$-\frac{U(\beta_{sm}, \gamma_{sm})}{kT} = (\lambda_2 P_2(\cos \beta_{sm}) + \lambda_4 P_4(\cos \beta_{sm}) + \epsilon (D_{02}^2(\beta_{sm}, \gamma_{sm}) + D_{0-2}^2(\beta_{sm}, \gamma_{sm}))) \quad (8)$$

where the coefficients λ_2 , λ_4 , and ϵ can be dependent on temperature but are independent of the excitation and emission wavelengths. The use of this maximum entropy form of the potential implies that the order parameters $\langle P_2 \rangle$, $\langle P_4 \rangle$, and $\langle D_{02}^2 \rangle$ are considered to be the most significant in the description in the orientational order of the perylene molecules. Note that the potential, eq 8, reduces to a cylindrically symmetric form ($\langle D_{02}^2 \rangle \equiv 0$) on setting $\epsilon = 0$.

Finally, we stress that the orientation of the transition dipole moments is taken to be independent of temperature, while the dynamic and orientational properties are considered to be independent of the excitation and emission wavelengths. These assumptions form the minimal globalizations applied.

Specific Models for $U(\Omega_{sm})$. A. *One-Population Models.* In these models the perylene molecule experiences the same orienting potential in every region of the bilayer. Thus, the following parameters enter the description of the anisotropy decay at temperature T : $\lambda_2(T)$, $\lambda_4(T)$, $\epsilon(T)$, $D_\perp(T)$, $D_\parallel/D_\perp(T)$, $\alpha_\mu(\lambda_{\text{ex}} = 256)$, $\alpha_\mu(\lambda_{\text{ex}} = 410)$, and $\alpha_\nu(\lambda_{\text{em}} = 470)$. Since measurements were carried out for 6 temperatures, this means

that a maximum number of 33 parameters need to be optimized. This number can be reduced by imposing additional restrictions on the orienting potential or by introducing further globalizations (e.g., a specific dependence of a parameter on temperature). We have tried various potentials corresponding to different physical situations.

One potential is the pure P_2 potential:

$$U(\beta_{sm}) = -kT(\lambda_2 P_2(\cos \beta_{sm}))$$

Perylene is thus considered to be a perfect disc; $\langle D_{02}^2 \rangle \equiv 0$. If no further globalization is applied, 21 adjustable parameters enter the GTA analysis.

A second potential is the P_2 - P_4 potential:

$$U(\beta_{sm}) = -kT(\lambda_2 P_2(\cos \beta_{sm}) + \lambda_4 P_4(\cos \beta_{sm}))$$

Again, $\langle D_{02}^2 \rangle \equiv 0$. The fourth-rank term allows a collective tilt in the orientational distribution. Twenty-seven adjustable parameters enter the GTA analysis in this case.

The third potential is the P_2 - D_{02}^2 potential:

$$U(\beta_{sm}, \gamma_{sm}) = -kT(\lambda_2 P_2(\cos \beta_{sm}) + \epsilon(D_{02}^2(\beta_{sm}, \gamma_{sm}) + D_{0-2}^2(\beta_{sm}, \gamma_{sm})))$$

Now the perylene disk is assumed to be rectangular with D_{2h} symmetry. The deviation from disk shape is reflected by the nonzero value of $\langle D_{02}^2 \rangle$. Twenty-seven parameters are needed as for the case of the $\langle P_2 \rangle$ - $\langle P_4 \rangle$ potential above.

B. Two-Population Models. The basic premise of these models is that the effective potential experienced by the perylene molecules depends on their depth in the bilayer relative to the aqueous interfaces. Here, we shall only deal with the simplest implementation of the idea by assuming that a fraction f of the molecules experiences a potential $U^1(\beta_{sm}, \gamma_{sm})$ while the fraction $(1 - f)$ experiences the potential $U^2(\beta_{sm}, \gamma_{sm})$. Both populations have distinct rotational diffusion coefficients, $D_{\perp,1}(T)$, $D_{\parallel,1}(T)$ and $D_{\perp,2}(T)$, $D_{\parallel,2}(T)$, respectively, though the fluorescence lifetime τ and the orientations of the transition dipole moments in the molecular frame are the same for both populations. The following set of parameters is now necessary for the description of the anisotropy decay: f , $\lambda_{2,1}(T)$, $\lambda_{4,1}(T)$, $\epsilon_1(T)$, $D_{\perp,1}(T)$, $(D_{\parallel}/D_{\perp})_1(T)$, $\lambda_{2,2}(T)$, $\lambda_{4,2}(T)$, $\epsilon_2(T)$, $D_{\perp,2}(T)$, $(D_{\parallel}/D_{\perp})_2(T)$, $\alpha_{\mu}(\lambda_{\text{ex}} = 256)$, $\alpha_{\mu}(\lambda_{\text{ex}} = 410)$, and $\alpha_{\nu}(\lambda_{\text{em}} = 470)$.

For pure P_2 potential for both populations,

$$U^1(\beta_{sm}) = -kT(\lambda_{2,1} P_2(\cos \beta_{sm})) \quad \text{with } \lambda_{2,1} \leq 0$$

$$U^2(\beta_{sm}) = -kT(\lambda_{2,2} P_2(\cos \beta_{sm})) \quad \text{with } \lambda_{2,2} \geq 0$$

Now a maximum of 40 parameters is needed for the analysis.

For the P_2 - D_{02}^2 potential for both populations,

$$U^1(\beta_{sm}, \gamma_{sm}) = -kT(\lambda_{2,1} P_2(\cos \beta_{sm}) + \epsilon_1(D_{02}^2(\beta_{sm}, \gamma_{sm}) + D_{0-2}^2(\beta_{sm}, \gamma_{sm}))) ; \lambda_{2,1} \leq 0$$

$$U^2(\beta_{sm}, \gamma_{sm}) = -kT(\lambda_{2,2} P_2(\cos \beta_{sm}) + \epsilon_2(D_{02}^2(\beta_{sm}, \gamma_{sm}) + D_{0-2}^2(\beta_{sm}, \gamma_{sm}))) ; \lambda_{2,2} \geq 0$$

In this case a maximum of 52 parameters are needed in principle.

Results

Total Fluorescence Intensity Decay. The total fluorescence intensity decay $F(t) = I_{\text{VV}}(t) + 2I_{\text{VH}}(t)$ is excellently described by a single exponential. The lifetime is independent of the

TABLE 1: Lifetime of Perylene in POPC Vesicles (1:500) at Various Temperatures^a

temp (°C)	fluorescence lifetime (ns)	temp (°C)	fluorescence lifetime (ns)
10	6.25	25	6.12
15	6.21	30	6.09
20	6.16	35	6.05

^a The lifetimes do not depend on excitation wavelength. The error in the temperature is 0.1°, while the error in the lifetimes is 0.1%.

TABLE 2: $r(0)$ for Perylene in POPC Vesicles (1:500) at Various Temperatures and Two Excitation Wavelengths^a

temp (°C)	$r(0)$ $\lambda_{\text{ex}} = 256 \text{ nm}$	$r(0)$ $\lambda_{\text{ex}} = 414 \text{ nm}$
10	-0.10	0.27
15	-0.08	0.25
20	-0.07	0.23
25	-0.06	0.22
30	-0.04	0.21
35	-0.03	0.21

^a The error in the temperature is 0.1 °C. The error in the value of $r(0)$ is 1%.

excitation wavelength but shows a slight dependence on temperature. The same lifetimes are recovered in the various model fits and are summarized in Table 1.

Anisotropy Decay. Model-Free Analysis. A multiexponential, model-free analysis reveals that the lowest global χ^2 possible is 1.41. The values of $r(0)$ at the various temperatures and for a certain combination of excitation and emission wavelengths are summarized in Table 2. The values extracted for $r(\infty)$ at all excitation wavelengths and temperatures range between -0.03 and 0.03.

One-Population Models. 1. Pure P_2 Potential. The fit procedure was started by analyzing the data with the maximum number of parameters required by the potential, 21 in the case under consideration. However, during the fit it appeared that certain parameters exhibited a negligible dependence on temperature. This finding was exploited for globalization. With this potential the ratio D_{\parallel}/D_{\perp} turned out to be independent of temperature and was thus globalized. Consequently, only 16 parameters were used, yielding a global χ^2 found of 1.82. All further attempts at globalization with other parameters resulted in a sharp increase of $\chi^2 > 10$.

Two classes of solutions with the same χ^2 were found: one class with a positive value of $\langle P_2 \rangle$ and the other with negative $\langle P_2 \rangle$ values. The values of all the other parameters are exactly equal. The absolute values of the order parameter were significantly larger than zero. The values of $r(0)$ calculated from the directions of the absorption and emission transition dipole moments were significantly lower than those extracted in the model-free analysis.

2. P_2 - P_4 Potential. Exactly the same physical solutions were found in this case as for the pure $\langle P_2 \rangle$ potential. Again D_{\parallel}/D_{\perp} could be globalized and the same value for χ^2 , 1.8, was recovered. Thus, 22 model parameters enter the analysis. Consequently, this model provides no more information than the $\langle P_2 \rangle$ model above and we shall not consider it any further.

3. P_2 - D_{02}^2 Potential. For this potential we find $\chi^2 = 1.42$, using all 27 parameters. All attempts at globalization resulted in a sharp increase of χ^2 . Sixteen statistically equivalent solutions are obtained that can be divided into four classes of four solutions each. The multiplicity within each class of solution arises from the inherent symmetry of a rectangular, flat molecule and reflects the ambiguity in assigning the x and y axes in the molecular plane. Two classes of the four have a

TABLE 3: Anisotropy Fit Results for the Two-Population Model Using the $\langle P_2 \rangle$ Potential

$\alpha_{\mu}(\lambda_{\text{ex}} = 256)$	$(97.9 \pm 0.2)^{\circ}$
$\alpha_{\mu}(\lambda_{\text{ex}} = 410)$	$(0 \pm 0.1)^{\circ}$
$\alpha_{\nu}(\lambda_{\text{em}} = 470)$	$(27.5 \pm 0.2)^{\circ}$
contribution of population 1 (f)	$(10.0 \pm 0.2)\%$
$\langle P_2 \rangle$	0.0020 ± 0.002
D_{\perp}	$0.016 + 0.0007(T - 10^{\circ}) \text{ ns}^{-1}$
D_{\parallel}/D_{\perp}	1.23 ± 0.03
contribution of population 2 ($1 - f$)	90%
$\langle P_2 \rangle$	-0.35 ± 0.02
D_{\perp}	$0.064 + 0.004(T - 10^{\circ}) \text{ ns}^{-1}$
D_{\parallel}/D_{\perp}	11.37 ± 0.02

negative value for $\langle P_2 \rangle$, $\langle P_2 \rangle = -0.40$, but differ only in the sign of the value of $\langle D_{02}^2 \rangle = \pm 0.20$. The change in sign of $\langle D_{02}^2 \rangle$ simply reflects an interchange of the x and y axes of a rectangular molecule.^{55,61} The other two classes are characterized by a positive value for $\langle P_2 \rangle$, $\langle P_2 \rangle = 0.3$, and again differ only in the sign of $\langle D_{02}^2 \rangle = \pm 0.16$.

Two Population Models. 1. P_2 Potentials. Using the maximum number of fit parameters (40), we found that for both populations $\langle P_2 \rangle$ and D_{\parallel}/D_{\perp} are independent of temperature. Furthermore, the individual diffusion coefficients D_{\perp} appear to exhibit a linear dependence on temperature. This finding allowed us to reduce the number of model parameters from the maximum of 40 to only 12. Remarkably, the lowest possible value of χ^2 , 1.42, was found using this reduced parameter set.

The parameters recovered from the analysis are shown in Table 3. The values of $r(0)$ calculated from the recovered orientations of the transition moments are identical with those obtained from the model-free analysis (Table 2).

2. $P_2 - D_{02}^2$ Potentials. The introduction of $\langle D_{02}^2 \rangle$ yielded no further improvement in the fits, and moreover, the recovered value of $\langle D_{02}^2 \rangle$ was zero at all temperatures. Apparently, all the information contained in the anisotropy decays can be extracted with the simple P_2 potentials.

Discussion

It is known that monomeric perylene exhibits a monoexponential fluorescence intensity decay in a wide variety of systems, while the presence of aggregates normally results in a complex decay behavior of the total fluorescence intensity. The observed monomeric lifetimes are independent of excitation and emission wavelengths and show only a weak dependence on the surrounding matrix. They are 4.0 ns in polymer films, 4.5–5.0 ns in isotropic solutions, 5.5 ns in liquid crystalline systems, and 6.0–6.5 ns in lipid bilayers.^{43–47} The last values are in excellent agreement with the value found here (Table 1). The observed fluorescence intensity decay thus indicates that perylene is indeed present in a purely monomeric form in the POPC vesicles and, moreover, that no quenching, for instance, by statistical traps,⁵³ takes place.

It is known that the absorption dipole moment at 410 nm and the emission moment at 470 nm are almost parallel,⁶⁰ $r(0) = 0.35 \pm 0.01$. Here, we find significantly lower values, in the range 0.27–0.21, which moreover decrease on raising the temperature (Table 2). A similar discrepancy is found for excitation at 256 nm. Now we expect⁶⁰ $r(0) = -0.12 \pm 0.02$ but find it to be in the range -0.10 to -0.03 , dependent on temperature.

Two different processes can be invoked in order to explain the reduction in $r(0)$. The first is the presence of very fast and efficient intermolecular energy transfer. Given that the Förster distance R_0 for perylenes is about 35 Å,⁶² energy transfer of sufficient efficiency will only take place if the perylene molecules are closely packed. This situation, however, is conducive to the formation of statistical pairs and for the self-

quenching of the fluorescence intensity by traps, resulting in a nonexponential decay of the fluorescence intensity.⁵³ Consequently, it can be ruled out in view of the observation of a monoexponential lifetime decay in each of our measurements.

The second mechanism for explaining the low values of $r(0)$ is averaging by restricted subnanosecond reorientational motions outside the time window of our experiments. The amplitude and rates of these motions are expected to increase with temperature, thus leading to a further reduction in the value of $r(0)$. This is in fact in line with our observations, and the explanation is supported by the MCD simulations presented in the preceding paper.

It thus appears that the best a GTA approach to the fluorescence anisotropy can achieve is the recovery of the effective values of $r(0)$ extracted from a model-free fit. Hence, only an effective orientation of the emission dipole moment in the molecular frame can be recovered.

The information about the orientational order and rotational dynamics of the perylene molecules can only be extracted from the anisotropy decay curves by fitting to the predictions of models for this behavior. We have here used rotational diffusion models employing a variety of orienting potentials. Each potential was found to yield a reasonable reproduction of the experimental data. The question now arises as to whether we can in fact choose among the potentials in an objective way.

It is clear that the single-population P_2 potential yields a fit of the data with a significantly higher value of χ^2 than that found with the model-free approach, 1.8 vs 1.4. Furthermore, the values of $r(0)$ recovered with this potential are lower than those found in the model-free fit. A close examination of the autocorrelation functions of the residuals for the fits to the individual decay curves indicates that the P_2 potential is not as successful as the model-free approach in describing the anisotropy decays.

In contrast the $P_2 - D_{02}^2$ potential yields a minimal χ^2 value similar to that of the model-free fit. The improvement in the fit relative to that of the P_2 potential may be simply due to the larger number of model parameters, 27 vs 16. Nevertheless, the extra parameters are introduced to account for the rectangular shape of the perylene molecules. The deviation from a disk shape is reflected in the value of the biaxial order parameter $\langle D_{02}^2 \rangle$, which we find to be significantly different from zero. A nonzero biaxiality for perylene was also found previously in nematic and isotropic liquid crystals.⁶³

We shall now address the physical significance of the two different, but statistically equivalent, classes of solutions, one with a positive $\langle P_2 \rangle$ and one with a negative $\langle P_2 \rangle$ found with the $P_2 - D_{02}^2$ potential. In view of the fact that $\langle P_2 \rangle$ is determined by the orientational distribution of the z -axis of the perylene model, solutions with negative values of $\langle P_2 \rangle$ corresponding to the perylene molecules are interdigitated between the lipid molecules, with their planes aligned parallel to their hydrocarbon chains (see the preceding paper for a detailed discussion). The solutions with the positive $\langle P_2 \rangle$ correspond to perylene molecules oriented with their plane parallel to the bilayer surface and, as shown in the preceding paper, located in the middle of the bilayer.

The results obtained with the $P_2 - D_{02}^2$ potential are ambiguous in that we have no criteria for choosing between the two physically distinct orientational distributions. It is thus not clear to what extent single-population models describe the behavior of perylene molecules in the bilayer. For this reason we shall now examine the two-population models suggested by the MCD simulations in order to see whether they offer a resolution of the problem. The two-population models are nothing more than

a synthesis of the two physical solutions found above with every single-population model.

The analysis reveals two additional advantages of the two-population model. In the first place, the analysis can be carried out with a significantly reduced parameter set compared to the single-population models. In the second place, the model yields values of $r(0)$ at both excitation wavelengths in good agreement with the values found in the model-free fit.

The analysis of the anisotropy decay using the two-population P_2 potentials model reveals that perylene is distributed into an oriented population and a randomly oriented one, each with its own diffusion coefficients. Surprisingly, the planar perylene molecules in the oriented fraction are found to undergo a highly anisotropic motion ($D_{\parallel} \gg D_{\perp}$), while those in the unoriented fraction undergo an almost isotropic diffusion. This difference is a strong indication of problems in the resolution of the experimental anisotropy decay into the components characterizing each fraction. Indeed, the simulations presented in the preceding paper question the reliability of the extracted information about the unoriented population. It was shown that synthetic anisotropy decays generated using equally weighted populations, $f = 1/2$, but with $\langle P_2 \rangle$ values of equal magnitude but opposite signs, are fitted by the two-population model in terms of an oriented and an unoriented population. The latter population has a significantly lower weight than the former and exhibits isotropic diffusion. This result of the analysis thus corresponds closely to the finding reported here. It is highly likely that perylene is partitioned into two populations in the bilayer. These populations have different orientational and reorientational properties. But since no independent information about the exact distribution of the molecules over the bilayer is available, the results of the GTA remain ambiguous.

Acknowledgment. We gratefully acknowledge HCM CT93 282 for support and for a fellowship to M. van Zandvoort. The SRS (Synchrotron Radiation Source, Daresbury, U.K.) was made available by an agreement between SERC (Scientific and Engineering Research Council) and NWO (Netherlands Organization for Scientific Research). We thank M. de Jong-Verheijden for preparing many of the samples. R. Tarroni and C. Zannoni thank CNR and MURST.

References and Notes

- Zannoni, C.; Arconi, A.; Cavatorta, P. *Chem. Phys. Lipids* **1983**, *32*, 179.
- van Langen, H.; Engelen, D.; van Ginkel, G.; Levine, Y. K. *Chem. Phys. Lett.* **1987**, *138*, 99.
- van Langen, H.; van Ginkel, G.; Levine, Y. K. *Liq. Cryst.*, submitted.
- van Langen, H.; van Ginkel, G.; Shaw, D.; Levine, Y. K. *Eur. Biophys. J.* **1989**, *17* (1), 37.
- van Langen, H.; Schrama, C.A.; Ranke, G.; van Ginkel, G.; Levine, Y. K. *Biophys. J.* **1989**, *55* (5), 937.
- Wratten, M. L.; van Ginkel, G.; van't Veld, A. A.; Bekker, A.; van Faassen, E. E.; Sevanian, A. *Biochemistry* **1992**, *31*, 10901.
- Verhagen, J. C. D.; ter Braake, P.; Teunissen, J.; van Ginkel, G.; Sevanian, A. *J. Lipid Res.* **1996**, *37*, 1488.
- Muller, J. M.; van Ginkel, G.; van Faassen, E. E. *Biochemistry* **1995**, *34*, 3092.
- Muller, J. M.; van Faassen, E. E.; van Ginkel, G. *Chem. Phys.* **1994**, *185*, 393.
- Eviatar, H.; van der Heide, U.; Levine, Y. K. *Mol. Eng.* **1995**, *5*, 195.
- Parassi, T.; Conti, F.; Glaser, M.; Gratton, E. *J. Biol. Chem.* **1984**, *259*, 14011.
- Grell, E. *Membrane Spectroscopy*; Springer-Verlag: Berlin, 1981.
- Cevc, G.; Marsh, D. *Phospholipid bilayers: physical principles and models*; Wiley: New York, 1987.
- Parasassi, T.; De Stasio, G.; Rush, R. M.; Gratton, E. *Biophys. J.* **1991**, *59*, 466.
- Davenport, L.; Dale, R. E.; Bisby, R. H.; Cundall, R. B. *Biochemistry* **1985**, *24*, 4097.
- van Ginkel, G.; Korstanje, L. J.; van Langen, H.; Levine, Y. K. *J. Chem. Phys.* **1986**, *81*, 49.
- Gratton, E.; Parasassi, T. *J. Fluoresc.* **1995**, *5* (1), 51.
- Toptygin, D.; Brand, L. *J. Fluoresc.* **1995**, *5* (1), 39.
- Stubbs, C. D.; Ho, C.; Slater, S. J. *J. Fluoresc.* **1995**, *5* (1), 19.
- Davenport, L.; Targowski, P. *J. Fluoresc.* **1995**, *5* (1), 9.
- Epard, R. M. *J. Fluoresc.* **1995**, *5* (1), 3.
- Rubsamen, H.; Barald, P.; Podleski, T. *Biochim. Biophys. Acta* **1976**, *523*, 767.
- Lakowicz, J. R.; Knutson, J. R. *Biochemistry* **1980**, *19*, 905.
- Chong, P. L.-G.; van der Meers, B. W.; Thompson, T. E. *Biochim. Biophys. Acta* **1985**, *813*, 253.
- Lakowicz, J. R.; Cherec, H.; Maliwal, B. P.; Gratton, E. *Biochemistry* **1985**, *24*, 376.
- Johansson, L. B. Å. *Chem. Phys. Lett.* **1985**, *118* (5), 516.
- Catalano, D.; Corrado, A.; Veracini, C. A.; Shilstone, G. N.; Zannoni, C. *Liq. Cryst.* **1989**, *4* (2), 217.
- Levine, Y. K.; van Ginkel, G. *The Molecular Dynamics of Liquid Crystals*; Kluwer Academic Publishers: The Netherlands, 1994; Chapter 22.
- Arcioni, A.; Tarroni, R.; Zannoni, C. *J. Chem. Soc., Faraday Trans.* **1991**, *87* (15), 2457.
- van Langen, H.; Levine, Y. K.; Ameloot, M.; Pottel, H. *Chem. Phys. Lett.* **1987**, *140*, 394.
- Ivanov, E. N. *Sov. Phys. JETP* **1964**, *18*, 1041.
- Roberts, J.; Lynden-Bell, R. M. *Mol. Phys.* **1971**, *21*, 689.
- Nordio, P.-L.; Segre, U. *The Molecular Physics of Liquid Crystals*; Academic Press: New York, 1979.
- Luckhurst, G. R.; Setaka, M.; Zannoni, C. *Mol. Phys.* **1974**, *28*, 49.
- Nordio, P.-L.; Busolin, P. *J. Chem. Phys.* **1971**, *55*, 5485.
- van der Heide, U. A.; Eviatar, H.; Levine, Y. K. *Handbook of Nonmedical Applications of Liposomes*; CRC Press: New York, 1996; Vol. III, Chapter 4.
- Kinosita, K., Jr.; Kawato, S.; Ikegami, A. *Adv. Biophys.* **1984**, *17*, 147.
- van der Sijts, D.A.; van Faassen, E. E.; Levine, Y. K. *Chem. Phys. Lett.* **1993**, *216*, 559.
- van der Heide, U. A.; van Zandvoort, M. A. M. J.; van Faassen, E. E.; van Ginkel, G.; Levine, Y. K. *J. Fluoresc.* **1993**, *3* (4), 269.
- van Gorp, M.; van Langen, H.; van Ginkel, G.; Levine, Y. K. *Polarized Spectroscopy of Ordered Systems*; Reidel: Dordrecht, 1988.
- van der Heide, U. A.; van Ginkel, G.; Levine, Y. K. *Chem. Phys. Lett.* **1996**, *253*, 118.
- Arcioni, A.; Tarroni, R.; Zannoni, C.; Dalcanale, E.; Du vosel, A. *J. Phys. Chem.* **1995**, *99*, 15981.
- Barkley, M. D.; Kowalczyk, A. A.; Brand, L. *J. Chem. Phys.* **1981**, *75* (7), 3281.
- Klein, U. K. A.; Haar, H. P. *Chem. Phys. Lett.* **1979**, *63* (1), 40.
- Mantulin, W. W.; Weber, G. *J. Chem. Phys.* **1977**, *66* (9), 4092.
- Johansson, L. B. Å.; Molotkovsky, J. G.; Bergelson, L. D. *J. Am. Chem. Soc.* **1987**, *109* (24), 7374.
- Tachikawa, H.; Faulkner, L. R. *Chem. Phys. Lett.* **1976**, *39* (3), 436.
- Arcioni, A.; Tarroni, R.; Zannoni, C. *J. Chem. Soc., Faraday. Trans.* **1993**, *89* (15), 2815.
- Ferguson, J. *J. Chem. Phys.* **1966**, *44* (7), 2677.
- Kimura, K.; Yamazaki, T.; Katsumata, S. *J. Phys. Chem.* **1971**, *75* (12), 1768.
- Vitukhnovsky, A. G.; Sluch, M. I.; Warren, J. G.; Petty, M. C. *Chem. Phys. Lett.* **1990**, *173* (5, 6), 425.
- Vitukhnovsky, A. G.; Sluch, M. I.; Warren, J. G.; Petty, M. C. *Chem. Phys. Lett.* **1991**, *184* (1-3), 235.
- van Zandvoort, M. A. M. J.; Wrobel, D.; Scholten, A. J.; de Jager, D.; van Ginkel, G.; Levine, Y. K. *Photochem. Photobiol.* **1993**, *58* (4), 600.
- Rose, M. E. *Elementary Theory of Angular Momentum*; Wiley: New York, 1957.
- van Zandvoort, M. A. M. J.; Wrobel, D.; Lettinga, P.; van Ginkel, G.; Levine, Y. K. *Photochem. Photobiol.* **1995**, *62* (2), 299.
- Levine, R. D.; Bernstein, R. B. *Modern Theoretical Chemistry, Volume III. Dynamics of Molecular Collisions*; Plenum: New York, 1975.
- van Gorp, M.; Levine, Y. K. *Chem. Phys. Lett.* **1991**, *180* (4), 349.
- van Gorp, M. *Colloid Polym. Sci.* **1995**, *273*, 607.
- Tarroni, R.; Zannoni, C. *J. Chem. Phys.* **1991**, *95*, 4550.
- Szubiakowski, J.; Balter, A.; Nowak, W.; Kowalczyk, A.; Wiśniewski, K.; Wierzbowska, M. *Chem. Phys.* **1996**, *208*, 283.
- Zannoni, C. *The Molecular Dynamics of Liquid Crystals*; Kluwer Academic Publishers: The Netherlands, 1994; Chapter 2.
- Kalman, B.; Johansson, L. B. Å.; Lindberg, M.; Engström, S. *J. Am. Chem. Soc.* **1989**, *93* (26), 181.
- Catalano, D.; Corrado, A.; Veracini, C. A.; Shilstone, G. N.; Zannoni, C. *Liq. Cryst.* **1989**, *4* (2), 217.